Proc. Natl. Acad. Sci. USA
Vol. 81, pp. 6728–6732, November 1984
Cell Biology

Introductory analysis of the GTP-cap phase-change kinetics at the end of a microtubule

(aggregation/polymer in solution/polymer on site/steady-state distribution)

TERRELL L. HILL

Laboratory of Molecular Biology, National Institute of Arthritis, Diabetes, and Digestive and Kidney Diseases, National Institutes of Health, Bethesda, MD 20205

Contributed by Terrell L. Hill, July 9, 1984

ABSTRACT **An introductory analysis is provided for the two-phase macroscopic kinetic model of the end of a microtubule. Some general relations are derived for one end of a very long microtubule in solution but the main results refer to the steady-state properties of microtubules grown on nucleated sites, as in the experiments of Mitchison and Kirschner [Mitchison, T. & Kirschner, M. W. (1984) *Nature (London)*, in press]. The two-phase model makes it possible to understand qualitatively how long microtubules can grow well below the critical concentration and also how grown microtubules can rapidly disappear from a nucleated site by shortening following a phase change.**

This paper presents some introductory analytical results relating to the existence of two different "phases" on the end of a microtubule (MT) (or actin filament): the MT end may be capped with GTP (the growing phase) or not capped (the shortening phase). An introduction to this subject is provided by ref. 1, which in turn is related to the recent experimental work of Mitchison and Kirschner (2, 3). For background and comparison, we begin with a few results from the much simpler theory, some of it well known, for an equilibrium or conventional steady-state (4) polymer.

Aggregation of a Conventional Polymer on a Nucleated Site

Consider the simple kinetic scheme in Fig. 1*a* for the aggregation of a polymer onto a nucleated site (Fig. 1*b*). The polymer size is m and P_m is the probability of size m; P_0 is the probability of an empty site. Both λ and λ' are first-order rate constants; $\lambda = \lambda^* c$, where c is the free monomer concentration. In an equilibrium polymer, the λ,λ' processes are true inverses of each other; in a steady-state polymer (4), for example Fig. 1*c*, the on (λ) and off (λ') processes are *not* inverses of each other. However, the same kinetic scheme can be used for both cases. There is no problem in making the first on rate constant (for $0 \rightarrow 1$) different from the other on constants (5), but we do not bother with this complication here. At steady state (or equilibrium), from Fig. 1*a*,

$$P_1 = (\lambda/\lambda')P_0, \qquad P_2 = (\lambda/\lambda')^2 P_0, \qquad \text{etc.} \qquad [1]$$

There is a finite attached polymer when $\lambda < \lambda'$. When $\lambda = \lambda'$, the polymer becomes infinitely long. When $\lambda > \lambda'$, the polymer grows at the rate $J = \lambda - \lambda'$. The concentration at which λ becomes equal to λ' is the critical concentration c_o: $\lambda^* c_o = \lambda'$. Hence, λ/λ' in Eq. **1** is c/c_o. From Eq. **1**, we find that

$$P_m = \left(1 - \frac{c}{c_o}\right)\left(\frac{c}{c_o}\right)^m, \qquad m = \frac{1}{1 - (c/c_o)}, \qquad [2]$$

The publication costs of this article were defrayed in part by page charge payment. This article must therefore be hereby marked "*advertisement*" in accordance with 18 U.S.C. §1734 solely to indicate this fact.

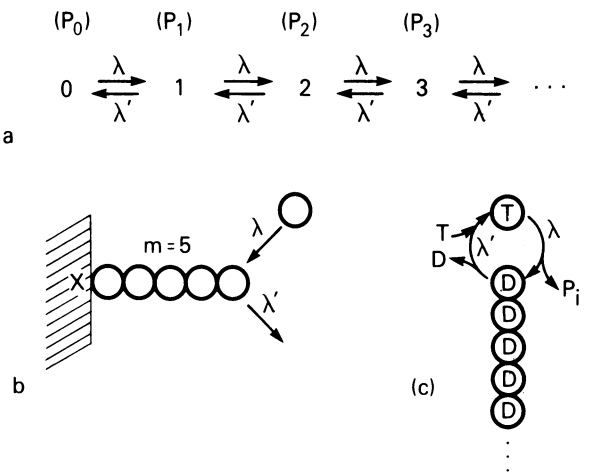

FIG. 1. (*a* and *b*) Models for aggregation of a simple polymer on a nucleated site. (*c*) Details of NTPase activity at the tip of a steady-state polymer.

where $\bar{m}$ is the mean size of polymers with $m \geq 1$. The mean polymer size becomes large only when c/c_o is very close to unity; $\bar{m} \rightarrow \infty$ when $c \rightarrow c_o$.

If we define P_{occ} as the probability that the site is occupied by a polymer of size larger than m_o (i.e., $m > m_o$), then, from Eq. **2**,

$$P_{occ} = (c/c_o)^{m_o+1}. \qquad [3]$$

This quantity is of interest if, for example, it takes a polymer of size greater than m_o to be detected visually (by electron microscope, say). A numerical example is shown in the lower right-hand corner of Fig. 2, where we have chosen (see below) $c_o = 2.432\ \mu M$ and $m_o = 100$. Both m and P_{occ} rise very steeply near $c = c_o$ but are very small otherwise. These conventional curves, together with the c/c_o line in the figure, are very different from the corresponding two-phase curves discussed below.

Transient at c Near c_o. If, at $t = 0$, we start with a large ensemble of attached polymers (as in Fig. 1*b*), all with $m = m^*$, and if c is held constant and close to c_o ($c < c_o$) so that large values of m predominate in the steady-state finally reached, then how does $P(m)$, treated as a continuous variable, evolve with time (starting from the δ function at $m = m^*$)? There is diffusion in the space of Fig. 1*a*, with "reflection" at the origin. The differential equation in P is

$$\frac{\partial P}{\partial t} = D\frac{\partial^2 P}{\partial m^2} - J\frac{\partial P}{\partial m} \qquad [4]$$

$$D \equiv (\lambda + \lambda')/2, \qquad J \equiv \lambda - \lambda' = \lambda^* c - \lambda', \qquad [5]$$

Abbreviation: MT, microtubule.

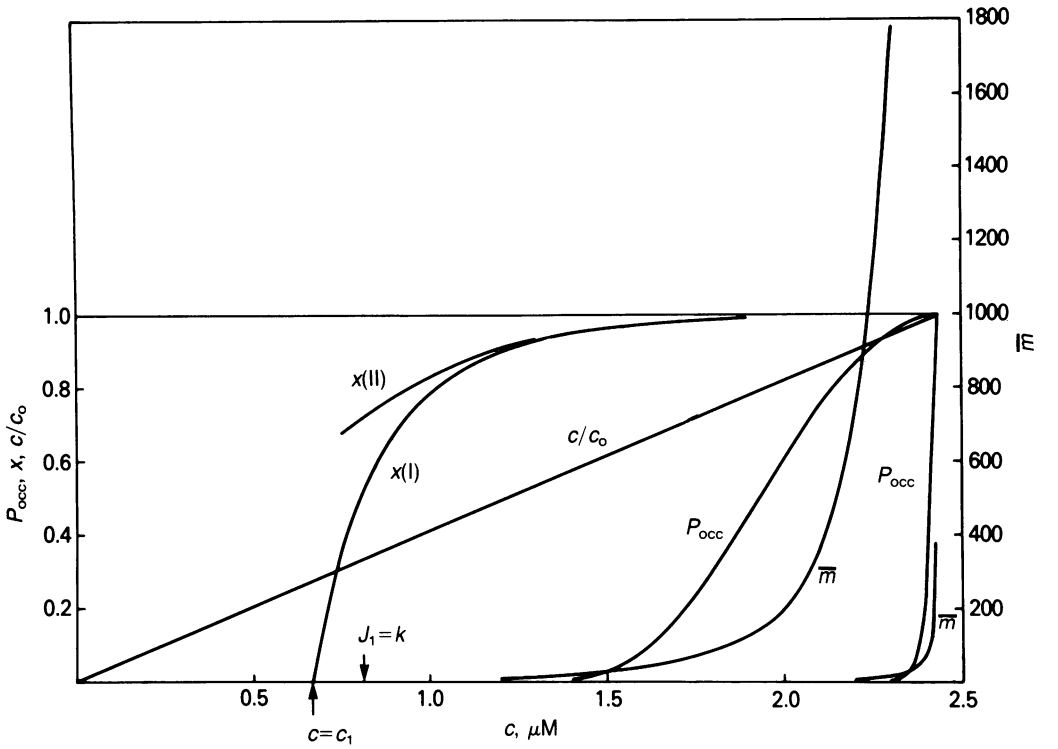

FIG. 2. The two curves in the lower-right corner and the c/c_o line relate to Eqs. **2** and **3** for a simple polymer (Fig. 1), with $m_o = 100$ and $c_o = 2.432$ μM. The remaining curves in the figure relate to a numerical example of a two-phase attached polymer, cases I and II (Eqs. **35–54**).

where D is the diffusion coefficient and $J < 0$ is the mean subunit flux. The solution is (6)

$$P(m, t; m^*) = \frac{1}{2(\pi Dt)^{1/2}}\left\{\exp\left[-\frac{(m - m^* - Jt)^2}{4Dt}\right] + \exp\left[\frac{-4m^*Jt - (m + m^* - Jt)^2}{4Dt}\right]\right\} - \frac{J}{D}\varphi\left(\frac{m + m^* + Jt}{(2Dt)^{1/2}}\right)e^{Jm/D}, \quad [6]$$

where

$$\varphi(x) \equiv \frac{1}{(2\pi)^{1/2}}\int_x^\infty e^{-y^2/2}dy. \quad [7]$$

At steady state ($t \to \infty$),

$$P(m, \infty; m^*) = -(J/D)e^{Jm/D}. \quad [8]$$

This agrees with Eq. **2** when c is close to c_o ($\bar{m}$ large).

If there is a distribution in m^* at $t = 0$, Eq. **6** is simply averaged over this distribution at any t. Note that Eq. **8** is independent of m^*. Equations **4–8** are related to dilution experiments (already grown polymers are suddenly switched to a free monomer concentration c).

Rearrangement of Length Distribution in Solution

Suppose, at $t = 0$, we have an ensemble of equilibrium or conventional steady-state (4) polymer molecules of length m^* in solution at the critical concentration for the two-ended polymer molecules. As time passes, the polymer length distribution $P(m)$ spreads from the δ function at $m = m^*$. Some polymers will shorten until disappearance. We assume no homogeneous nucleation of new polymers on the time scale considered here. The kinetic scheme is shown in Fig. 3; polymers have $m \geq 2$. The two polymer ends are designated α and β; the off rate constants at the two ends are λ'_α and λ'_β. At the critical concentration, the total on rate is equal to the total off rate, $\lambda'_\alpha + \lambda'_\beta$. The diffusion equation in this case (with zero net subunit flux) is

$$\frac{\partial P}{\partial t} = D\frac{\partial^2 P}{\partial m^2}, \qquad D = \lambda'_\alpha + \lambda'_\beta. \quad [9]$$

This is one-dimensional diffusion with "absorption" essentially at the origin $m = 0$ (m is generally large). Polymer molecules that shorten to disappearance put monomers into solution that contribute to the lengthening of the surviving polymers; the free monomer concentration remains constant at the critical concentration (see below).

The length distribution at t is (see equation 24 in ref. 7)

$$P(m, t; m^*) = \frac{1}{2(\pi Dt)^{1/2}}\left\{\exp\left[-\frac{(m - m^*)^2}{4Dt}\right] - \exp\left[-\frac{(m + m^*)^2}{4Dt}\right]\right\}. \quad [10]$$

The fraction of surviving polymer molecules at t is then found to be

$$p(t; m^*) = \int_0^\infty P dm = \frac{1}{(2\pi)^{1/2}}\int_{-m^*/(2Dt)^{1/2}}^{m^*/(2Dt)^{1/2}} e^{-x^2/2}dx. \quad [11]$$

This function starts ($t = 0$) at unity and, after a lag period

$$\underset{}{\overset{\lambda'_\alpha+\lambda'_\beta}{\longleftarrow}}\ 2\ \underset{\lambda'_\alpha+\lambda'_\beta}{\overset{\lambda'_\alpha+\lambda'_\beta}{\rightleftarrows}}\ 3\ \underset{\lambda'_\alpha+\lambda'_\beta}{\overset{\lambda'_\alpha+\lambda'_\beta}{\rightleftarrows}}\ 4\ \underset{\lambda'_\alpha+\lambda'_\beta}{\overset{\lambda'_\alpha+\lambda'_\beta}{\rightleftarrows}}\ \cdots$$

FIG. 3. Model for a two-ended (α and β) simple polymer in solution at the critical concentration. The polymer disappears as a consequence of the final transition on the left.

that depends on m^*, falls eventually to zero as $t \to \infty$. The total amount of polymer (and hence free monomer) remains constant:

$$\int_0^\infty mPdm = m^*. \quad [12]$$

If there is a distribution in m^* (which can have the effect of reducing the lag), one simply averages p, above, over this distribution. For example, for a flat initial distribution in the range $0 \leq m^* \leq m_{max}$,

$$\bar{p}(t) = \frac{1}{m_{max}} \int_0^{m_{max}} p(t; m^*)dm^*. \quad [13]$$

The above equations have been applied by Carlier *et al.* (8) to sonicated actin polymers.

While it is appropriate to use rate constants in Fig. 1*a* that are independent of m, this is an approximation for small m (9, 10) in the case of free polymers in solution (Fig. 3).

One End of a Very Long Two-Phase Polymer

We turn now to the two-phase model introduced in the previous paper (figure 2 of ref. 1). In this section, some general introductory relations for one end (either α or β) of a very long polymer molecule in solution are derived. The kinetic scheme is shown in Fig. 4. The variable m counts subunits added to or lost from only the one end (e.g., we might start, at $t = 0$, with $m = 0$; m can be negative here). The states in phase 1 (or 2) have probabilities P_m (or R_m). We define $f_1 = \Sigma P_m$ and $f_2 = \Sigma R_m$, with $f_1 + f_2 = 1$. Thus, f_1 is the fraction of polymer ends in phase 1, etc. From Fig. 4,

$$dP_m/dt = \lambda P_{m-1} + \lambda' P_{m+1} + k'R_m - (\lambda + \lambda' + k)P_m \quad [14]$$

$$dR_m/dt = \mu R_{m-1} + \mu' R_{m+1} + kP_m - (\mu + \mu' + k')R_m. \quad [15]$$

Because of the large range in m in cases of interest, the continuous version of Eqs. **14** and **15** is important:

$$\frac{\partial P}{\partial t} = D_1 \frac{\partial^2 P}{\partial m^2} - J_1 \frac{\partial P}{\partial m} + k'R - kP \quad [16]$$

$$\frac{\partial R}{\partial t} = D_2 \frac{\partial^2 R}{\partial m^2} - J_2 \frac{\partial R}{\partial m} + kP - k'R, \quad [17]$$

where

$$J_1 = \lambda - \lambda', \quad J_2 = \mu - \mu', \quad D_1 = (\lambda + \lambda')/2, \quad D_2 = (\mu + \mu')/2. \quad [18]$$

Eqs. **16** and **17** (compare Eq. **4**) are one-dimensional diffusion equations in P and R with added terms arising from phase changes (k, k'). The center of the P distribution moves to the right in Fig. 4 ($J_1 > 0$) and spreads as it moves (D_1); the R distribution moves to the left ($J_2 < 0$) and spreads (D_2); but this behavior is perturbed by the two distributions leaking into each other (k, k').

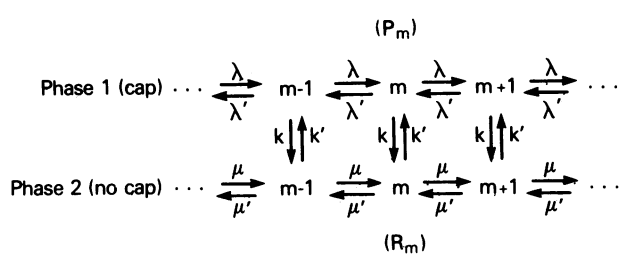

FIG. 4. Kinetic scheme for one end of a very long two-phase polymer in solution.

We return now to the more general Eqs. **14** and **15**. By summing these equations over m as they stand, or summing after multiplying by m or m^2, a number of relations are easy to derive. Direct summation gives

$$df_1/dt = k'f_2 - kf_1, \quad df_2/dt = kf_1 - k'f_2. \quad [19]$$

The solution, if c is held constant, is

$$f_1(t) = f_1^\infty + (f_1^0 - f_1^\infty)e^{-(k+k')t}$$
$$f_1^\infty = k'/(k + k'), \quad f_2 = 1 - f_1, \quad [20]$$

where f_1^0 and f_1^∞ are the initial and final values of f_1.

We define the mean values of m:

$$\bar{m} = \sum_m m(P_m + R_m) = f_1\bar{m}_1 + f_2\bar{m}_2 \quad [21]$$

$$\bar{m}_1 = \sum_m mP_m/f_1, \quad m_2 = \sum_m mR_m/f_2. \quad [22]$$

The latter are the means in the separate phases. On multiplying Eqs. **14** and **15** by m and summing, we find

$$d\bar{m}/dt = f_1J_1 + f_2J_2 \equiv J \quad [23]$$

$$d\bar{m}_1/dt = J_1 + (k'f_2/f_1)(\bar{m}_2 - \bar{m}_1) \quad [24]$$

$$d\bar{m}_2/dt = J_2 + (kf_1/f_2)(\bar{m}_1 - \bar{m}_2). \quad [25]$$

If f_1 and f_2 have reached their steady-state values (Eq. **20**), Eq. **23** becomes

$$\frac{d\bar{m}}{dt} = J = \frac{k'J_1 + kJ_2}{k + k'}, \quad [26]$$

as in equations **4** and **5** of ref. 1. J is now a constant and $\bar{m} = Jt + \bar{m}^0$. Also, in Eqs. **24** and **25**,

$$k'f_2/f_1 \to k, \quad kf_1/f_2 \to k'. \quad [27]$$

At large t, both $\bar{m}_1$ and $\bar{m}_2$ behave like $\bar{m}$ (above) and maintain a constant difference:

$$\bar{m}_1 - \bar{m}_2 \to (J_1 - J_2)/(k + k'). \quad [28]$$

The variance in m, and related quantities, is defined by

$$\sigma^2 = \overline{m^2} - \bar{m}^2, \quad \sigma_1^2 = \overline{m_1^2} - m_1^2, \quad \sigma_2^2 = \overline{m_2^2} - \bar{m}_2^2$$

$$\overline{m_1^2} = \sum_m m^2P_m/f_1, \quad \overline{m_2^2} = \sum_m m^2R_m/f_2$$
$$\overline{m^2} = f_1\overline{m_1^2} + f_2\overline{m_2^2} \quad [29]$$

$$\sigma^2 = f_1\sigma_1^2 + f_2\sigma_2^2 + f_1f_2(\bar{m}_1 - \bar{m}_2)^2.$$

Then, on multiplying Eqs. **14** and **15** by m^2 and summing over m, we derive

$$d\sigma^2/dt = 2[f_1D_1 + f_2D_2 + f_1f_2(J_1 - J_2)(\bar{m}_1 - \bar{m}_2)] \quad [30]$$

$$d\sigma_1^2/dt = 2D_1 + (k'f_2/f_1)[\sigma_2^2 - \sigma_1^2 + (\bar{m}_1 - \bar{m}_2)^2] \quad [31]$$

$$d\sigma_2^2/dt = 2D_2 + (kf_1/f_2)[\sigma_1^2 - \sigma_2^2 + (\bar{m}_1 - \bar{m}_2)^2]. \quad [32]$$

Two-Phase Polymer on a Nucleated Site

A centrosome or axoneme presents nucleated sites on which MTs can grow (2, 3). The two-phase model applied to any one of these MTs has the kinetic diagram (figure 5 of ref. 1) shown in Fig. 5. State 0 is the empty site. The polymer size is m, with probabilities P_m (phase 1) and R_m (phase 2). Growth can be initiated ($m = 0 \rightarrow 1$) only in the growing phase (capped; phase 1). Eq. **14** still applies for $m \geq 1$ and Eq. **15** applies for $m \geq 2$. The other needed relations for the analysis of Fig. 5 are

$$dP_0/dt = \lambda' P_1 + \mu' R_1 - \lambda P_0 \quad [33]$$

$$dR_1/dt = \mu' R_2 + kP_1 - (\mu + \mu' + k')R_1. \quad [34]$$

The differential equations **16** and **17** are also pertinent for large nucleated polymers; there is reflection into phase 1 at the origin ($m = 0$). However, we confine ourselves in this paper to a discussion of the steady-state ($t = \infty$) solution of Eqs. **14**, **15**, **33**, and **34**; that is, we put all $dP_m/dt = 0$ and $dR_m/dt = 0$. The subunit flux is zero.

Because k and k' in Fig. 5, in cases of interest here, are small compared with the other rate constants (1), the *steady-state* solution is hardly affected (see below) if we replace λ,λ' by the unidirectional composite J_1 and/or μ,μ' by the composite $-J_2$, as shown in Fig. 6. Both J_1 and $-J_2$ are positive. The model in Fig. 6 is especially useful because its mathematical properties are so simple. (In practice, it may not be possible to decompose J_2 into μ and μ' in any case.) We discuss and compare four cases below (the first three prove to be slight approximations to the fourth):

I. In Fig. 5, $\lambda' \rightarrow 0$, $\mu \rightarrow 0$, $\lambda \rightarrow J_1$, $\mu' \rightarrow -J_2$ (Fig. 6).
II. In Fig. 5, $\mu \rightarrow 0$, $\mu' \rightarrow -J_2$.
III. In Fig. 5, $\lambda' \rightarrow 0$, $\lambda \rightarrow J_1$.
IV. Fig. 5, unchanged.

We consider case I first (Fig. 6) and in most detail. The steady-state solution of Eqs. **14**, **15**, **33**, and **34** is easily found to be

$$P_m = P_0 x^m, \qquad R_m = J_1 P_0 x^{m-1}/-J_2 \quad [35]$$

$$P_0 = -J_2(1 - x)/(J_1 - J_2) \quad [36]$$

$$x \equiv J_1(k' - J_2)/-J_2(k + J_1). \quad [37]$$

The sum $P_m + R_m$ is the probability of a polymer with m subunits. The normalization relation is

$$P_0 + \sum_m P_m + \sum_m R_m = P_0 + f_1 + f_2 = 1. \quad [38]$$

Note that both P_m and R_m resemble P_m in Eq. **2**; x here is analogous to c/c_o in Eq. **2**. However, because k and k' are

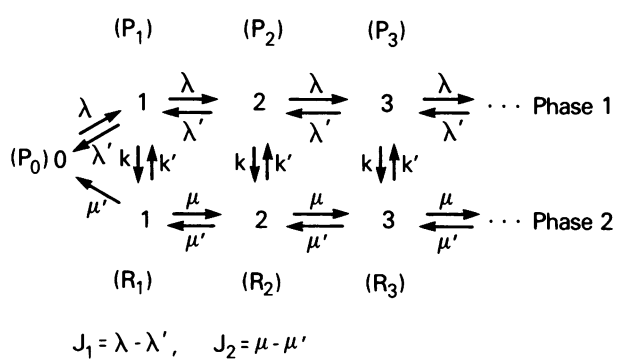

FIG. 5. Kinetic scheme for a two-phase polymer aggregating on a nucleated site. This scheme is referred to as case IV in the text.

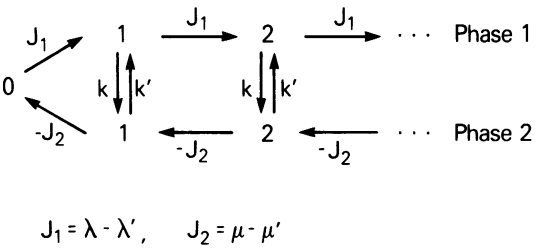

FIG. 6. Simplified version of Fig. 5 in which composite Js are used. This is referred to as case I in the text.

relatively small in Eq. **37**, x is near unity. To illustrate this, we use the same numerical example (from Monte Carlo printouts) introduced in figures 3 and 4 of ref. 1. This provides concentration dependences of all rate constants. The curve labeled x(I) in Fig. 2 shows $x(c)$ calculated from Eq. **37** for this example. This x is very close to unity over a considerable range in c, unlike the corresponding c/c_o in the same figure (for the aggregation of a conventional polymer). Where x is near 1, P_m and R_m fall off very slowly with increasing m. This was the basis of the approximate argument in equations **8** and **9** of ref. 1, which provides a qualitative understanding of the odd behavior of this two-phase model. In this connection, note that Eq. **37** gives, for k and k' small,

$$1 - x \cong \frac{k}{J_1} - \frac{k'}{(-J_2)}. \quad [39]$$

This is related to equation **9** of ref. 1 (see Eq. **44** below).

The probabilities P_m and R_m converge in Eq. **35** for $x < 1$. At $x = 1$, infinite polymers are formed. This locates the critical concentration c_o. On putting $x = 1$ in Eq. **37**, we find that

$$k'J_1 = k(-J_2) \text{ at } c = c_o, \quad [40]$$

as in ref. 1. Note, from Eq. **26**, that $J = 0$ at $c = c_o$ for the end of a long polymer molecule in solution (i.e., the same free end would have the same c_o whether the polymer is attached or not).

Other properties in case I are as follows:

$$f_1 = \sum_m P_m = P_0 x/(1 - x) \quad [41]$$

$$f_2 = \sum_m R_m = J_1 P_0/-J_2(1 - x) \quad [42]$$

$$f_1/f_2 = P_m/R_m = (k' - J_2)/(k + J_1) \cong -J_2/J_1 \quad [43]$$

$$\overline{m} = 1/(1 - x), \qquad \sigma^2/\overline{m}^2 = x \quad [44]$$

$$P_{\text{occ}} = (J_1 - J_2 x)x^{m_o}/(J_1 - J_2) \cong x^{m_o+1}, \quad [45]$$

where $\overline{m}$ is the mean size of polymers with $m \geq 1$ and P_{occ} is the probability that $m > m_o$, just as in Eqs. **2** and **3**. Also, note that f_1/f_2 in Eq. **43** for the free end of an *attached* polymer is different (except at $c = c_o$) from $f_1/f_2 = k'/k$ for an end of a very long polymer molecule in solution under steady conditions (Eq. **20**).

The above algebra is still simple if the first on rate constant ($0 \rightarrow 1$) in Fig. 6 differs from the others (J_1). But we omit details.

To illustrate numerically, Fig. 2 includes (for the numerical example referred to above) $\overline{m}$ and P_{occ} (with $m_o = 100$) as functions of c ($c_o = 2.432$ μM, from ref. 1). P_{occ} corresponds to Fig. 4 of Mitchison and Kirschner (2). These curves are strikingly different from those in the lower-right corner of Fig. 2 for a conventional nucleated polymer with the same c_o

(chosen to facilitate comparison). The two-phase behavior (with reflection into phase 1 at the origin) allows long but finite attached aggregates to exist in a range of c above $c_1(J_1 = 0)$ but far below $c = c_o$. Incidentally, $f_1 \cong 1$ (phase 1 dominates in the time average) over the whole range of calculation in Fig. 2 for an attached steady-state polymer (Eq. **43**), because $-J_2 >> J_1$, but this is not true of f_1 for the corresponding end of a long polymer in solution, at steady state with respect to the phase transition (see figure 4 of ref. 1 and Eq. **20** here).

The resemblance of P_{occ} to Fig. 4 of ref. 2 would be much closer if a much larger $J_1(c)$ had been used. Such a $J_1(c)$ was in fact found by Mitchison and Kirschner (2). Qualitatively, what the analysis of the model suggests is that, well above $c = c_1$ and well below c_o, a nucleated site can, at a slow rate, grow a long capped MT because k is very small. But when the phase change ($1 \rightarrow 2$) finally occurs, the uncapped MT shortens rapidly, quite possibly to disappearance (because k' is also small). The empty site thus formed can then start the process over again. The equations above provide the *average* steady-state properties of the MT on a site.

Further comments on Fig. 2: $x \cong 1/2$ when $J_1 = k$ (because k' is very small); $m_o = 100$ was chosen because this approximate size (for a single helix out of five) is needed for detection (2, 3); figure 4 of Mitchison and Kirschner (2) does not reach full saturation at $c = c_o$, as P_{occ} does in Fig. 2, probably because a true steady state has not yet been reached.

We turn now to case II. This case is important because of the practical difficulty of separating J_2 into μ and μ'. Case II is similar to case I. The main properties are found to be as follows:

$$P_m = P_0 x^m, \qquad R_m = (P_0/y)x^m \qquad (m \geq 1) \qquad [46]$$

$$P_0 = (1 - x)y/(x + y) \qquad [47]$$

$$f_1 = xy/(x + y), \qquad f_2 = xy/(x + y)y \qquad [48]$$

$$f_1/f_2 = P_m/R_m = y \qquad [49]$$

$$\overline{m} = 1/(1 - x), \qquad \sigma^2/\overline{m}^2 = x \qquad [50]$$

$$P_{occ} = (1 + y)x^{m_o+1}/(x + y), \qquad [51]$$

where

$$x = \frac{\lambda'(k' - J_2) - J_2(k + \lambda) - \sqrt{\ }}{-2\lambda' J_2} \qquad [52]$$

$$y = \frac{\lambda'(k' - J_2) + J_2(k + \lambda) + \sqrt{\ }}{2\lambda' k} \qquad [53]$$

$$\sqrt{\ } = [J_2^2(k + \lambda)^2 + 2\lambda' J_2(\lambda - k)(k' - J_2) + \lambda'^2(k' - J_2)^2]^{1/2}. \qquad [54]$$

The critical concentration $c = c_o$, defined at $x = 1$, occurs when $-J_2 k = (\lambda - \lambda')k'$, as expected (here also $J = 0$ in Eq. **26**). In the numerical example in Fig. 2, the P_{occ} and $\overline{m}$ curves are unchanged (on this scale), but there is an alteration in x, denoted x(II) in the figure, at low c (where k is no longer small).

In case III, there is no simple analytical solution and there is no x variable as above (e.g., in Eq. **46**) except asymptotically for large enough m. However, the P_m and R_m are easy to calculate successively, starting, say, with $P_0 \equiv 1$ (normalization is postponed to the end).

In case IV, the successive calculation of the P_m and R_m cannot be done directly as in case III; an iteration procedure must be used. Again there is an asymptotic x for large m.

Cases III and IV were compared numerically with cases I and II in a similar but different example in which empirical analytical functions were used for all rate constants. Suffice it to say that, for all practical numerical purposes, in the range of c of interest ($1.4 \leq c \leq c_o$), the four models are essentially equivalent. The conclusion is that the simple case I (Fig. 6) is an excellent approximation to case IV (Fig. 5) and might as well be used for *steady states* provided that k and k' are small (x near 1). Case II, as well as case I, might be important for transients.

Probability of Disappearance of Attached Polymer

If we start with an attached polymer of size m^*, in case I (Fig. 6) above and it is *growing* (i.e., in phase 1), what is the probability it will disappear (reach $m = 0$) after $\nu = 1, 3, 5, \ldots$ phase changes? Omitting details for lack of space, we find for this probability

$$\Omega_\sigma^+ = \frac{a}{A}\left(\frac{ab}{A^2}\right)^\sigma e^{-bm^*} \sum_{\rho=0}^{\sigma} \frac{(\rho + 1)(2\sigma - \rho)!(Am^*)^\rho}{(\sigma + 1)!(\sigma - \rho)!\rho!} \qquad [55]$$

$$a = k/J_1, \qquad b = k'/-J_2, \qquad A = a + b, \qquad \sigma = (\nu - 1)/2.$$

Similarly, if the initial polymer (m^*) is *shortening* (phase 2), the probability that the polymer will disappear after $\nu = 2, 4, \ldots$ phase changes is

$$\Omega_\sigma^- = \left(\frac{ab}{A^2}\right)^{\sigma+1} Am^* e^{-bm^*} \sum_{\rho=0}^{\sigma} \frac{(2\sigma - \rho)!(Am^*)^\rho}{(\sigma + 1)!(\sigma - \rho)!\rho!}, \qquad [56]$$

where $\sigma = (\nu/2) - 1$. For $\nu = 0$, the probability is e^{-bm^*}.

One (good) approximation was made in deriving Eqs. **55** and **56**: the number of subunits added (or lost) in time t is taken to be $J_1 t$ (or $-J_2 t$), not allowing for fluctuations. This is equivalent to assuming that, in phase 1 (for example), the probability that the phase change will occur after N subunits have been added can be approximated by

$$\left(\frac{J_1}{J_1 + k}\right)^N \left(\frac{k}{J_1 + k}\right) \cong \frac{k}{J_1} e^{-kN/J_1}. \qquad [57]$$

This is accurate if $J_1 >> k$.

The special case $m^* = 0$ in Eq. **55** is especially important:

$$\Omega_\sigma^+ = \frac{a}{A}\left(\frac{ab}{A^2}\right)^\sigma \frac{(2\sigma)!}{(\sigma + 1)!\sigma!} \qquad (m^* = 0). \qquad [58]$$

For example, in Fig. 2 at $c = 1.9\ \mu M$ (where $P_{occ} = 0.441$ and $\overline{m} = 124.0$), the probabilities of disappearance of a newly started ($m^* = 0$) aggregate after 1, 3, 5, ... phase changes are 0.9731 ($=\Omega_0^+$), 0.0255, 0.00134, 0.00009, ... Thus, the new polymer almost always disappears after only one phase change ($1 \rightarrow 2$)—that is, in the first shortening session. The values of Ω_0^+ at $c = 1.6$ and $2.2\ \mu M$ are 0.9934 and 0.8525, respectively. At $c = c_o$ ($2.432\ \mu M$), $a = b$ and $\Omega_0^+ = 0.50$. The probability of eventual disappearance ($\Sigma_\sigma \Omega_\sigma^+$) can be shown to be unity if $a \geq b$ ($c \leq c_o$) and a/b if $b > a$ ($c > c_o$).

1. Hill, T. L. & Chen, Y. (1984) *Proc. Natl. Acad. Sci. USA* **81**, 5772–5776.
2. Mitchison, T. & Kirschner, M. W. (1984) *Nature (London)*, in press.
3. Mitchison, T. & Kirschner, M. W. (1984) *Nature (London)*, in press.
4. Hill, T. L. & Kirschner, M. W. (1982) *Int. Rev. Cytol.* **78**, 1–125.
5. Hill, T. L. (1964) *Thermodynamics of Small Systems* (Benjamin, New York), Part 2, p. 78.
6. Cox, D. R. & Miller, H. D. (1965) *The Theory of Stochastic Processes* (Wiley, New York), p. 224.
7. Chandrasekhar, S. (1943) *Rev. Mod. Phys.* **15**, 1–89.
8. Carlier, M. F., Pantaloni, D. & Korn, E. D. (1984) *J. Biol. Chem.* **259**, 9987–9991.
9. Hill, T. L. (1980) *Proc. Natl. Acad. Sci. USA* **77**, 4803–4807.
10. Hill, T. L. (1981) *Biophys. J.* **33**, 353–371.